Journal of
Manufacturing and Materials Processing

MDPI

Article

Microstructural Characterization of Shrouded Plasma-Sprayed Titanium Coatings †

Hong Zhou [1,*], Zhi Liu [2] and Liancong Luo [3]

1 Centre for Engineering and Industrial Design, Waikato Institute of Technology, Hamilton 3240, New Zealand
2 Science and Technology Ltd., Hamilton 3210, New Zealand; cathy.zhi.liu@gmail.com
3 School of Resources, Environment and Geoscience, Yunnan University, Kunming 650091, China; freshwatermodeling@gmail.com
* Correspondence: zhouhong.nz@gmail.com; Tel.: +64-22-689-5586

† This manuscript is extension version of the conference paper: Zhou, H.; Liu, Z.; Luo, L. Microstructure and Phase Composition of Titanium Coatings Plasma Sprayed with a Shroud. In Proceedings of the International Conference on Materials Applications and Engineering 2017 (ICMAE2017), Qingdao, China, 25–27 August 2017.

Received: 5 December 2018; Accepted: 3 January 2019; Published: 10 January 2019

Abstract: Titanium and its alloys are often used for corrosion protection because they are able to offer high chemical resistance against various corrosive media. In this paper, shrouded plasma spray technology was applied to produce titanium coatings. A solid shroud with an external shrouding gas was used to plasma spray titanium powder feedstock with aim of reducing the oxide content in the as-sprayed coatings. The titanium coatings were assessed by optical microscope, scanning electron microscopy, X-ray diffraction, LECO combustion method and Vickers microhardness testing. The results showed that the presence of the shroud and the external shrouding gas led to a dense microstructure with a low porosity in the plasma-sprayed titanium coatings. The oxygen and nitrogen contents in the titanium coating were kept at a low level due to the shielding effect of the shroud attachment and the external shrouding gas. The dominant phase in the shrouded titanium coatings was mainly composed of α-Ti phase, which was very similar to the titanium feedstock powders. The shrouded plasma-sprayed titanium coatings had a Vickers microhardness of 404.2 ± 103.2 HV.

Keywords: shroud; plasma spray; titanium coatings; microstructure

1. Introduction

Titanium is not a rare substance, as it ranks as the ninth most plentiful element and the fourth most abundant structural metal in the Earth's crust [1]. However, the difficulty in processing makes the metal expensive. As light metals, titanium and titanium alloys provide high specific strength, exceptional biocompatibility, and excellent corrosion resistance, which make them widely applied in aircraft, chemical and marine engineering and medical devices [1–4]. Titanium and its alloys are now frequently used for corrosion protection because they are able to offer high chemical resistance against various corrosive media, especially chloride-containing solutions due to a dense self-sealing oxide layer formed immediately when exposed to an oxygen-containing atmosphere [5–7].

Coating technology has been developed to fulfill the industrial demands. This technology allows combining cheap structural materials with a thin layer of high value material [8–10]. Thermal spraying techniques are coating processes in which melted materials are sprayed onto a surface. There, the molten droplets flatten, rapidly solidify and form a deposit on structural materials. Consequently, the protective coatings of titanium combined with cheap bulk materials offering strength and ductility are supposed to provide sufficient protection and lower the cost. Titanium coatings may be applied in

marine engineering and the shipbuilding industry due to the excellent corrosion resistance to seawater. Its applications can also be found in the food industries and/or medical devices like clinical implants, thanks to its exceptional biocompatibility.

Atmospheric plasma spraying (APS), performed in ambient air, is a flexible coating technique that can be used with a wide range of coating materials to meet many different needs [11,12]. However, titanium is a very reactive metal at high temperatures due to its strong affinity with gases such as oxygen, nitrogen and hydrogen, which lead to a degradation in the coating properties. In order to prevent titanium from too much oxidation, the spray process has to be carried out in a vacuum or an inert atmosphere. Within the thermal spray area, low pressure plasma spray (LPPS) or vacuum plasma spray (VPS) has been the promising technique used for titanium deposition thanks to its inert atmosphere and ability to form dense coatings with low porosity and oxygen content [4]. Corrosion resistance similar to that of bulk Ti has been reported if proper spraying parameters, including the size of the feedstock powder, are optimized [10]. However, this process has limitations in terms of the size of the components and is rather expensive. The shrouded plasma spray process uses an attachment to shield the plasma jet as it exits the torch. An external gas shroud envelops the plasma jet as it leaves the attachment [13–18]. This is expected to be a cost effective method to produce titanium coatings with low oxide content.

In this paper, shrouded plasma spraying technology was used to deposit titanium coatings on mild steel substrates. The microstructure of titanium powders and coatings was investigated and characterized in terms of chemical composition, phase composition, porosity, microhardness, and microstructure.

2. Materials and Methods

Pure titanium powders from Xi'an Lilin International Trade Co., Ltd., Xi'an, China, were selected as the feedstock powders for the titanium coating fabrication. The titanium powders were made by hydride–dehydride (HDH) method. The chemical composition of the HDH Ti powder is shown in Table 1. The powder particle size and distribution was determined using a laser diffraction method (Malvern Mastersizer 2000, Malvern Instruments Ltd., UK), which relies on the fact that the diffraction angle is inversely proportional to the particle size.

Table 1. Chemical composition of the HDH titanium powders.

Element	H	O	N	C	Fe	Ti
HDH Ti powder (wt%)	0.23	0.35	<0.03	0.07	<0.11	Bal

A shroud attachment was designed for the plasma spraying of titanium coatings [10]. A SG-100 plasma gun (Praxair surface technologies, Danbury, CT, USA) with the shroud attachment was then used to do the plasma spray work with the HDH titanium powders, as shown in Figure 1. The plasma gun had a high-speed Mach II anode hardware with a forward injection internal powder injector and was mounted on a 6-axis robot which sprayed the samples in a raster pattern. Mild steel plates (100 × 25 × 3 mm) were used as the substrates which were degreased, and sand blasted before depositing titanium coatings onto them. The plasma spraying parameters are presented in Table 2.

Special attention was given to adjusting the powder carrier gas flow rate within the shroud to generate an inflight particle trajectory with a low angle of deviation from the central axis to prevent the build-up of powder on the inside wall of the shroud. The trial for spraying with the shroud used argon as an external shrouding gas at the exit with a flow rate of 300 slpm. After each argon shroud gas trial, the interior of the shroud was cleaned to leave a dust-free surface prior to the next trial.

Free stand titanium coating specimens were peeled off from the mild steel substrates, and then polished to remove the elements from the substrate. Quantitative chemical analysis (oxygen and nitrogen) for the titanium coatings was carried out at Durkee Testing Laboratories Inc., USA,

using a LECO combustion method, which incorporates gas fusion in a graphite crucible under a flowing inert gas stream (helium) and the measurement of combustion gases by infrared absorption and thermal conductivity. Following this fusion process, oxygen combines with carbon to form CO_2 and nitrogen is released as N_2.

Figure 1. The shroud attachment for plasma-sprayed titanium coatings.

Table 2. The plasma-spraying parameters for the titanium coatings with the shroud.

Spray Parameter	Setting
Current, A	800
Voltage, V	80
Primary gas, Argon, slpm	85
Auxiliary gas, Helium, slpm	18
Powder feed rate, g/min	30
Spray passes	10
Spray distance, mm	100
Transverse speed, mm/s	500

Scanning electron microscopes (SEM, Zeiss EVO 18, German, and Hitachi S4700, Japan) with second electron imaging were operated at 20 kV to observe the microstructures and morphologies of the power feedstock and coating specimens. Cross-sectional samples of titanium coatings were metallographically prepared by polishing for the microstructural analysis. An Olympus BX60 optical microscope equipped with a digital camera was used to capture images for the porosity analysis of the titanium coatings. Porosity is defined as the ratio of the total empty area to the total area. Five samples were investigated at a magnification of 150, and ten captured images were used for each sample. Porosity was then examined by using IQ image analysis software.

Phase transformations were studied using an X-ray diffractometer (XRD, Bruker, model D8, Germany) with CuKα radiation at 40 kV and 30 mA; the scanning speed of 2θ was 2° min^{-1} when measuring from 20°–80°. The angle of incidence α was 10°. In order to remove the effect of surface oxides and attempt to characterize the oxides within the bulk of the coatings, the sample surfaces were ground away and the XRD analysis was implemented on the ground surface.

A microhardness test was performed on 5 samples using a Vickers indenter (LECO, Michigan, USA) with a load of 300 g for 15 s on the coating's cross-sections. The cross-sections of the titanium coatings were polished before indentations, and the distance between two indentations was at least three times the diagonal to prevent stress-field effects from nearby indentations. The Vickers microhardness was averaged from 10 indents per sample.

3. Results and Discussion

3.1. Titanium Powders

The particle morphology of the HDH titanium powders is illustrated in Figure 2. From the SEM image, it can be seen clearly that the HDH titanium powders present irregular shapes with some sharp sides/ends. This was determined by the nature of the hydride–dehydride process, which was to resize large titanium pieces down to a finer particle size distribution through crushing, milling and screening. Powder flowability is the ability of a powder to flow. Generally, spherical powders possess good flowability, and for powders with irregular shape, flowability is often poor. Poor flowability will likely result in fluctuations in the powder feed rate and thus in an inhomogeneous coating structure. However, when exposed in the plasma flame after a few millimeters' trajectory, the particles will quickly melt and thus start to spheroidize [11,12]. Consequently, the effect of irregular particle shape on the capability to flow during the flight in the plasma jet will disappear. The size of the titanium particles in Figure 2 is between approximately 20–80 μm. Some small size (micrometer) titanium dust can be found on the surfaces of the titanium particles.

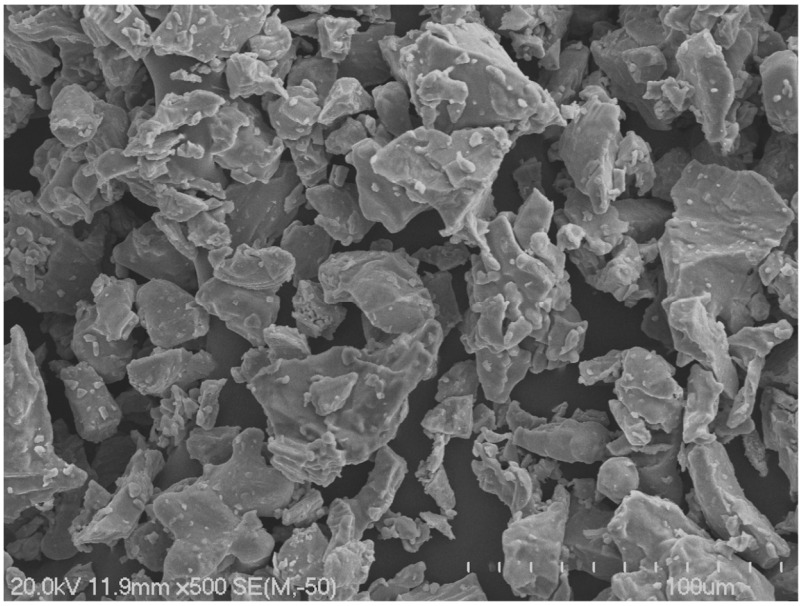

Figure 2. SEM image showing the particle morphology of the HDH titanium powders.

Figure 3 presents the particle size distribution of the HDH titanium powders. The d (0.1), d (0.5) and d (0.9) values for the titanium powders are summarized in Table 3. This analysis showed that the HDH titanium powder particles were mainly in the range of 10–120 μm; the mean particle size was 52.32 μm with 10% volume reported at 20.98 μm and 90% volume at 90.93 μm. The specific area of the titanium powder particles was 0.161 m^2/g. The results indicated that the powder particles had a relatively broad range of size distribution, at approximately 110 μm. However, over 50% of the titanium powder particles were in the size range 40–75 μm.

Powder feedstock morphologies and size distribution play important roles in microstructure and properties of plasma-sprayed coatings. Usually coarse powders produce a coarser and more openly-structured coating with less oxidation than fine powders, which is mainly due to the difference in the surface area of the powder particle. Meanwhile, the broader the size distribution, the more different the particle momentums at the injector exit, and thus the larger the particle trajectory distribution, resulting in a larger velocity and temperature distribution at impingement onto the substrate [12].

Table 3. The particle size distributions of the HDH titanium powders.

d (0.1), μm	d(0.5), μm	d(0.9), μm
20.986	47.777	90.931

Note: The d (0.1), d (0.5) and d (0.9) mean that 10%, 50% and 90% of the volume fraction of the powder particles have particle sizes (in micrometers) below a particular value, respectively.

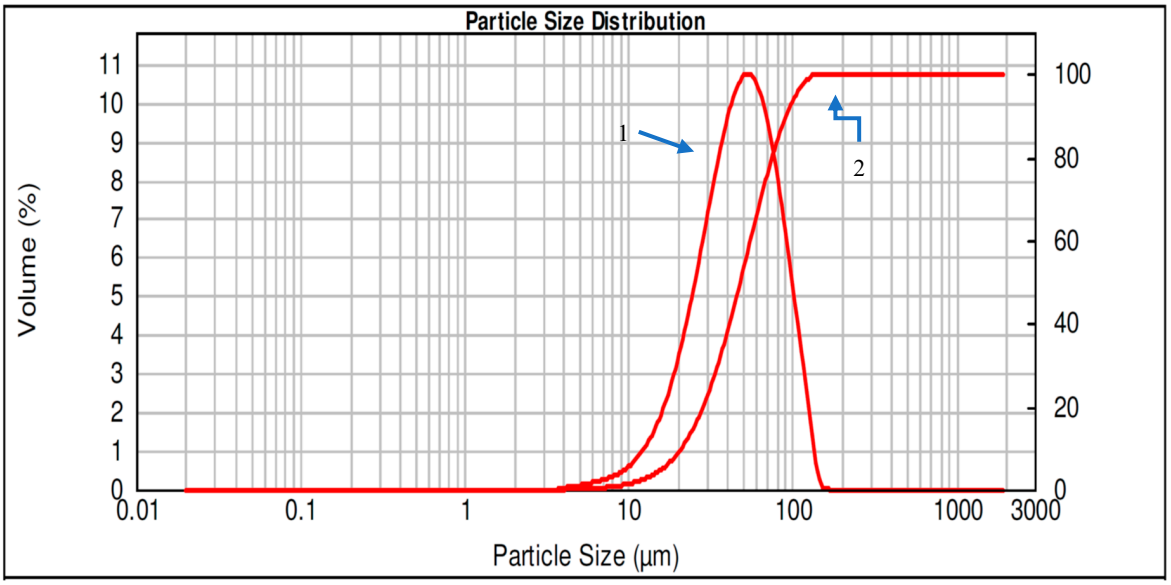

Figure 3. Particle size distributions for the HDH titanium powders. Curve (**1**) shows the volume percent at the corresponding particle size, and curve (**2**) shows the accumulated volume percent under the corresponding particle size.

The phase composition result of the X-ray diffraction analysis of the titanium feedstock powders is presented in Figure 4. From the XRD pattern, it was found that the HDH titanium powder was merely composed of a α-Ti phase. None of oxide peaks were observed in the pattern. Pure titanium crystallizes at low temperatures in a modified ideally hexagonal close packed structure, which has only three slip systems and a relatively poor plastic deformation ability in relation to the β-Ti phase with a body-centered cubic structure that is stable at high temperatures [1]. The oxidation level of titanium particles during their manufacturing process is an important issue to be considered because the oxide content in the titanium coatings is never lower than that of the sprayed particles.

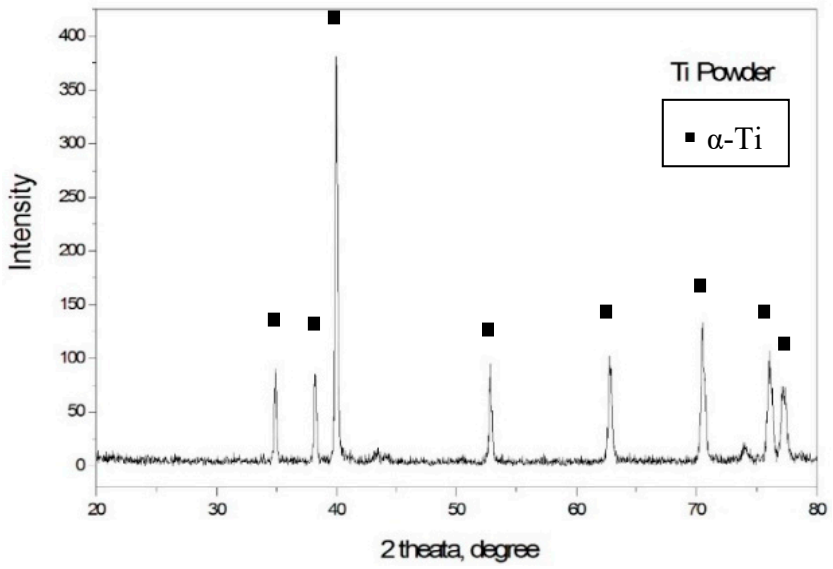

Figure 4. XRD pattern of the HDH titanium powders in the range 2θ = 20°–80°.

3.2. Titanium Coating Analysis

Figure 5 presents the SEM images of the titanium coatings. The polished cross-section of the titanium coating is shown in Figure 5a. The image reveals that the shrouded titanium coating had a dense microstructure with a low porosity. Images of the polished cross-sections of titanium coatings were also captured by the optical microscope with an integrated digital camera. Porosity distributions were then determined by using the IQ image analysis software. Special attention was required during metallographic preparation to prevent the pull-out of internal titanium oxides and splats. The porosities of the titanium coatings was 2.38 ± 0.31, which shows that the presence of the shroud and shroud gas flow led to a low porosity in the titanium coatings.

Figure 5b shows the fractured cross-section of the shrouded titanium coating. It can be clearly observed that there exists a lamellar structure, which is typical for a plasma-sprayed coating. The splats with thin thickness were in close contact with the titanium coating. A few of the voids in the splats and some porosity in between the splats could be seen. No unmelted particles were found in this shrouded titanium coating. As we know, in the plasma-spray process the feedstock powders were injected into a plasma flame, which was produced by the ionization of an inert gas. The plasma heated the titanium particles into a molten or semi-molten state. The particles then struck on the substrate, spread and quickly solidified. The impact of subsequent particles built up the titanium coating and formed the lamellar structure.

From the SEM images, we can see that the presence of the shroud and the external shrouding gas led to a dense lamellar microstructure with low porosity in the titanium coatings. This can be explained by the shrouded plasma-spray process. This process used the shroud attachment on the air plasma spray torch to modify the plasma flow. In principle, the attachment itself physically shielded the plasma jet as it exited the torch. An inert gas shroud like argon was then injected, enveloping the plasma jet as it left the shroud, preventing the molten particles from reaction with oxygen/nitrogen from ambient air, reducing the amount of entrainment of cold and heavy ambient air, and delaying the corresponding drop in temperature. Consequently, this retarded particle cooling. Meanwhile, gas-shrouded nozzles can extend the hot core of the jet by rearranging the gas flow to increase the dwell time of particles in the plasma [18]. Thus, the shroud was expected to generate better heating of the particles during the in-flight period. The greater extent of particle heating with the shroud led to better melting in the plasma jet, and more fully molten titanium particles were obtained, and splat spreading on the substrate could also be improved, which then contributed to a reduction in porosity and a dense lamellar structure.

a)

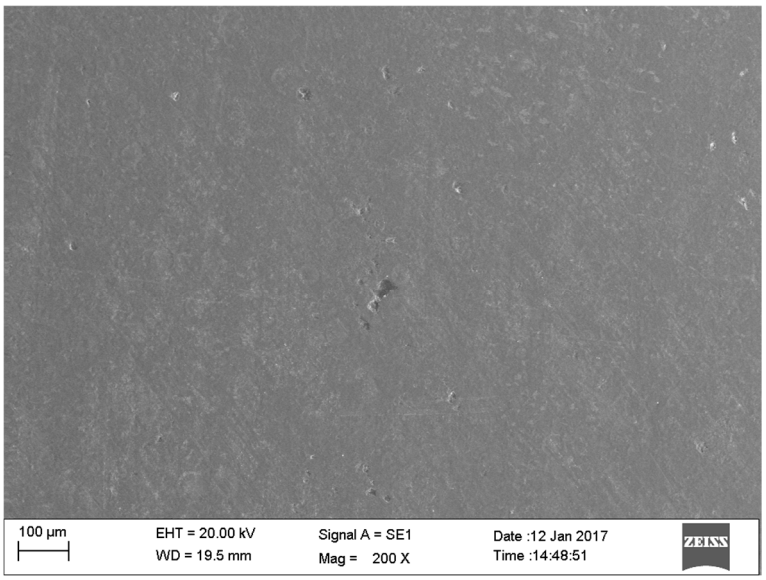

b)

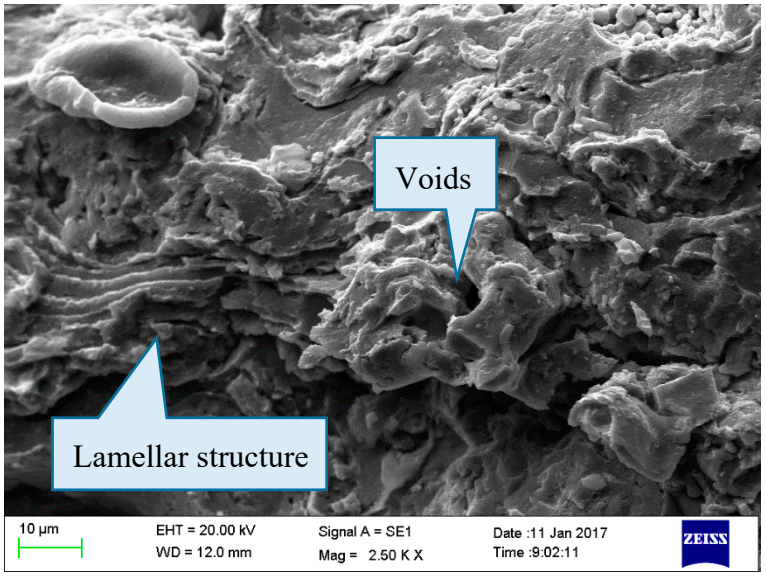

Figure 5. SEM images showing the shrouded plasma-sprayed Ti coatings. (**a**) the polished cross-section; (**b**) the fractured cross-section.

Quantitative chemical analysis using the combustion method was carried out for the shrouded titanium coatings. The oxygen and nitrogen contents are listed in Table 4. The result shows that both the oxygen and nitrogen contents in the titanium coating were still kept at a low level, but both increased after the coating deposition in relation to the titanium powders. The oxygen content increased from 0.35%wt to 0.76%wt. and the nitrogen content went up to 0.039%wt. The nitrogen content in the titanium coatings was much lower than the oxygen content.

Table 4. The oxygen and nitrogen contents in the as-sprayed titanium coatings.

Titanium Coatings	Oxygen, wt%	Nitrogen, wt%
Shrouded	0.76	0.039

Titanium will react with the oxygen and nitrogen to form the oxide of titanium and a TiN layer in the initial stages of oxidation when exposed to the surrounding air at high temperatures, and then TiN will be oxidized at around 800 °C in a normal atmosphere [19,20]. In the plasma spray process,

the titanium particles were accelerated and then fully or partially melted before impacting with the substrate where they were flattened, formed splats and built up a lamellar structure. The temperature in the plasma flame was so high that an in-flight particle reaction would occur. If cold air engulfed the plasma flame, the molecules of nitrogen and oxygen were subjected to thermal dissociation and became highly reactive monotonic atoms when heated by plasma. This resulted in the oxidation and nitridation of the titanium particles in the plasma spraying. However, the oxidation took priority over the nitridation of the titanium particles during the in-flight period, since titanium nitride oxidizes at high temperatures, and then turned into titanium oxide. In addition, titanium oxide and nitride also came into being during splat formation and the build-up of the coating because the temperature was still high at that moment.

The phase composition results for the titanium coating plasma-sprayed using the shroud are illustrated in Figure 6. The XRD pattern presents a similar curve as that for the pure titanium powder. The result reveals that the dominant phase in the titanium coating plasma-sprayed using the shroud was still the α-Ti phase. The broader width of those peaks indicate that a finer-grain microstructure in the as-sprayed titanium coating was obtained compared with the powder's XRD pattern. Furthermore, some very weak peaks for the titanium oxide and/or nitride can also be observed from this pattern, which means that there might exist a small trace of titanium oxide and/or nitride in the shrouded titanium coating. The quantity of titanium oxide and nitride in the shrouded coating might be very small, based on the low intensity peaks of titanium oxide/nitride in the XRD result. TiO_2 is usually present in nature rather than TiO because the monoxide can be readily oxidized to the dioxide when exposed to appreciable amounts of oxygen at high temperatures. However, for the as-sprayed shrouded titanium coatings in this study, the oxide consisted of only the monoxide phase of TiO. There are two possible factors causing this. The first factor is the inadequate amount of oxygen during the build-up of the coating due to the shielding effect of the shroud attachment and the inert gas shroud. The other is the rather short time that the titanium particle spent at a high temperature during the plasma spraying process, which was followed by a very fast cooling rate (10^5–10^6 Ks^{-1} range) [21,22] when the particles impacted on the substrate. Therefore, it resulted in the rapid formation of TiO other than TiO_2 in the as-sprayed titanium coatings. TiO can be fast growing and does not form protective titanium oxide scales.

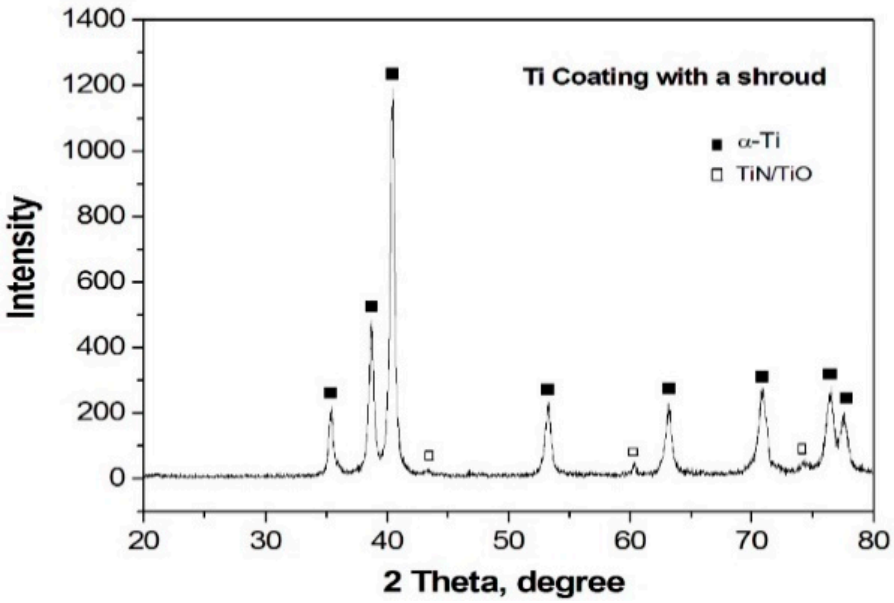

Figure 6. XRD pattern in the range of 2θ = 20°–80° of the titanium coatings plasma-sprayed using the shroud.

The microhardness was examined on the shrouded titanium coatings. The mean microhardness values were 404.2 ±103.2 HV. In general, plasma-sprayed coatings present high microhardness values due to the rapid cooling, oxidation, lamellar structure and residual stresses induced by the plasma spraying process. Meanwhile the oxygen/nitrogen content in titanium also has a significant effect on its mechanical properties due to embrittlement. Consequently, the microhardness is high in the plasma-sprayed titanium coatings. Further, the formation of titanium oxides/nitrides in the titanium coatings could also result in an increase in the microhardness.

4. Conclusions

This work presents the fabrication of titanium coatings by shrouded plasma spraying. Microstructural analyses of the shrouded titanium coatings were carried out.

Pure titanium powders with a particle size in the range of 10–120 μm were used for the fabrication of the titanium coating. A shroud attachment was designed for the plasma spraying process. The presence of the shroud and external shrouding gas led to a dense microstructure with a low porosity in the titanium coatings. The oxygen and nitrogen contents in the titanium coating were kept at a low level due to the shielding effect of the shroud. The dominant phase in the shrouded titanium coating was the α-Ti phase, which is similar to the titanium powders. The shrouded plasma-sprayed titanium coating had a Vickers microhardness of 404.2 ± 103.2 HV.

Author Contributions: Conceptualization, H.Z. and Z.L.; methodology, H.Z. and L.L.; formal analysis, H.Z.; Z.L.; data curation, H.Z. and Z.L.; writing—original draft preparation, H.Z.; writing—review and editing, H.Z. and Z.L.; supervision, H.Z.; project administration, H.Z.

Funding: This research was funded by contestable fund from Waikato Institute of Technology, Hamilton, New Zealand.

Conflicts of Interest: The authors declare no conflict of interest.

References

1. Peters, M.; Hemptenmacher, J.; Kumpfert, J.; Leyens, C. Structure and Properties of Titanium and Titanium Alloys. In *Titanium and Titanium Alloys: Fundamentals and Applications*; Leyens, C., Peters, M., Eds.; Wiley-VCH Verlag GmbH & Co. KGaA: Weinheim, Germany, 2005; pp. 1–36, Print ISBN 9783527305346, Online ISBN 9783527602117. [CrossRef]
2. Antunes, R.; Oliveiraa, M.; Salvador, C. Materials selection of optimized titanium alloys for aircraft applications. *Mater. Res.* **2018**, *21*, e20170979. [CrossRef]
3. Gangwar, K.; Ramulu, M. Friction stir welding of titanium alloys: A review. *Mater. Des.* **2018**, *141*, 230–255. [CrossRef]
4. Zhou, H.; Gabbitas, B.; Mathews, S.; Zhang, D. Titanium and titanium alloy coatings for corrosion protection. In Proceedings of the 12th World Conference on Titanium, V3, Beijing, China, 19–24 June 2012; pp. 1906–1910.
5. Kitashima, T.; Kawamura, T. Prediction of oxidation behavior of near-α titanium alloys. *Scr. Mater.* **2016**, *124*, 56–58. [CrossRef]
6. Bagot, P.; Radecka, A.; Magyar, A.; Dye, D.; Rugg, D. The effect of oxidation on the subsurface microstructure of a Ti-6Al-4V alloy. *Scr. Mater.* **2018**, *148*, 24–28. [CrossRef]
7. Satko, D.; Shaffer, J.; Tiley, J.; Semiatin, S.; Pilchak, A.; Kalidindi, S.; Kosaka, Y.; Glavicic, M.; Salem, A. Effect of microstructure on oxygen rich layer evolution and its impact on fatigue life during high-temperature application of α/β titanium. *Acta Mater.* **2016**, *107*, 377–389. [CrossRef]
8. Walker, M. Microstructure and bonding mechanisms in cold spray coatings. *Mater. Sci. Technol.* **2018**, *34*, 2057–2077. [CrossRef]
9. Naumenko, D.; Pillai, R.; Chyrkin, A.; Quadakkers, W. Overview on recent developments of bondcoats for plasma-sprayed thermal barrier coatings. *J. Therm. Spray Technol.* **2017**, *26*, 1743–1757. [CrossRef]
10. Zhou, H.; Liu, Z.; Luo, L. Microstructure and phase composition of titanium coatings plasma sprayed with a shroud. In Proceedings of the MATEC Web of Conferences, Qingdao, China, 25–27 August 2017.
11. Fauchais, P.; Vardelle, M.; Goutier, S. Latest researches advances of plasma spraying: From splat to coating formation. *J. Therm. Spray Technol.* **2016**, *25*, 1534–1553. [CrossRef]

12. Fauchais, P.; Montavon, G.; Bertrand, G. From powders to thermally sprayed coatings. *J. Therm. Spray Technol.* **2010**, *19*, 56–80. [CrossRef]
13. Matthews, S. Shrouded plasma spray of Ni-20Cr coatings utilizing internal shroud film cooling. *Surf. Coat. Technol.* **2014**, *249*, 56–74. [CrossRef]
14. Morks, M.; Berndt, C. Corrosion and oxidation properties of NiCr coatings sprayed in presence of gas shroud system. *Appl. Surf. Sci.* **2010**, *256*, 4322–4327. [CrossRef]
15. Kim, S.; Choi, S.; Kim, G.; Hong, S. Effects of shroud gas injection on material properties of tungsten layers coated by plasma spraying. *Thin Solid Film* **2010**, *518*, 6369–6372. [CrossRef]
16. Planche, M.; Liao, H.; Coddet, C. Oxidation control in atmospheric plasma spraying coating. *Surf. Coat. Technol.* **2007**, *202*, 69–76. [CrossRef]
17. Thomson, I.; Pershin, V.; Mostaghimi, J.; Chandra, S. Experimental testing of a curvilinear gas shroud nozzle for improved plasma spraying. *Plasma Chem. Plasma Process.* **2001**, *21*, 65–82. [CrossRef]
18. Jankovic, M.; Mostaghimi, J.; Pershin, V. Design of a new nozzle for direct current plasma guns with improved spraying parameters. *J. Therm. Spray Technol.* **2000**, *9*, 114–120. [CrossRef]
19. Milošv, I.; Strehblow, H.; Navinšek, B. Oxidation of ternary TiZrN hard coatings studied by XPS. *Surf. Interface Anal.* **1998**, *26*, 242–248. [CrossRef]
20. Milošv, I.; Strehblow, H.; Navinšek, B.; Metikoš-Huković, M. Electrochemical and thermal oxidation of TiN coatings studied by XPS. *Surf. Interface Anal.* **1995**, *23*, 529–539. [CrossRef]
21. Padture, N.; Gell, M.; Jordan, E. Thermal barrier coatings for gas-turbine engine application. *Science* **2002**, *296*, 280–284. [CrossRef] [PubMed]
22. Kotalík, P.; Voleník, K. Cooling rates of plasma-sprayed metallic particles in liquid and gaseous nitrogen. *J. Phys. D Appl. Phys.* **2001**, *34*, 567–573. [CrossRef]